

## ARTICLE

Influence of Pressure on  $\text{SiN}_x\text{:H}$  Film by LF-PECVD

Zhen-li Wen\*, Xiao-ning Cao, Chun-lan Zhou, Wen-jing Wang

*Key Laboratory Solar Thermal Energy and Photovoltaic Systems, Institute of Electrical Engineering, Chinese Academy of Sciences, Beijing 100190, China*

(Dated: Received on September 26, 2011; Accepted on November 28, 2011)

Hydrogenated silicon nitride films as an effective antireflection and passivation coating of silicon solar cell were prepared on p-type polished silicon substrate ( $1.0 \Omega\text{cm}$ ) by direct LF-PECVD (low frequency plasma enhanced chemical vapor deposition) of Centrotherm. The preferable passivation effect was obtained and the refractive index was in the range of 2.017–2.082. The refractive index of the hydrogenated silicon nitride films became larger with the increase of the pressure. Fourier transform infrared spectroscopy was used to study the pressure influence on the film structural properties. The results highlighted high hydrogen bond and high Si–N bonds density in the film, which were greatly influenced by the pressure. The passivation effect of the films was influenced by the Si dangling bonds density. Finally the effective minority lifetime degradation with time was shown and discussed by considering the relationship between the structural properties and passivation.

**Key words:**  $\text{SiN}_x\text{:H}$  thin film, Pressure, Passivation, Structural properties

## 1. INTRODUCTION

Solar cells are devices with a large surface-to-volume ratio, and their energy conversion efficiency may be severely influenced by surface recombination. Besides, compared with the electronic-grade silicon, solar-grade silicon contains lots of impurities and defects, which behave themselves as recombination centre and interact additionally with the crystallographic defects enhancing their recombination properties [1, 2]. So, low surface recombination velocity and improvements of bulk quality are key issues for efficiency improvements of silicon solar cells. Many techniques of passivation have been used to reduce surface recombination losses in the past few decades. So far, hydrogenated silicon nitride films by the plasma enhanced chemical vapour deposition (PECVD) have been widely used in industrial silicon solar cells [3]. The main advantages of the PECVD method are: low processing temperature ( $<500 \text{ }^\circ\text{C}$ ) [4], the possibility to tune the refractive index over a wide range of 1.8–2.3 and large concentration of hydrogen in the deposited layers [5].

For silicon solar cells, the refractive index of the film should be about 2.0 and the thickness should be required to meet the minimum reflectivity at the 600 nm wavelength [6]. These proper optical refractive index and thickness can be used as very effective antireflective coating, but the surface and bulk passivation effect provided by the layer should be more concerned. Gener-

ally speaking, the silicon passivation mechanism can be explained from two aspects: one is field-effect passivation and the other is hydrogen passivation effect. The high concentration of positive charge incorporated in the first 20 nm of the hydrogenated silicon nitride film forms an accumulation layer and causes band bending by means of field effect. The accumulation layer on the surface of  $n^+$  emitter, acting as ideally reflecting potential barrier for minority carriers, keeps them away from the surface, so the surface recombination will be reduced [7]. Surface passivating properties are generally considered to be affected by the refractive index and the structural properties [8]. The hydrogen in the film also can passivate defects and impurities segregated on extended defects in the silicon [3]. This passivation of silicon is fully achieved by a short anneal, namely the firing front side metallization, which drives the hydrogen from the silicon nitride layer into the silicon wafer [9]. The effect of bulk passivation depends not only on the hydrogen content of the film, but also on its structural properties and the anneal process [10]. Chemical, mechanical, optical and electrical properties of silicon nitride as well as the effectiveness of surface and bulk passivation strongly depend on the selected deposition technique and processing parameters.

In a lot of previous work [4, 11–15], the  $\text{SiN}_x\text{:H}$  films were mostly prepared by the small equipments suitable for lab purpose and were not suitable for industrial production. Once more, they were mostly focus on the influence of ammonia-to-silane gas flow ratio, plasma power, and temperature, and seldom on the influence of pressure. Some studies only gave the simple results of influence of pressure on deposition rate but not structure and passivation properties [15]. In this work, we

\* Author to whom correspondence should be addressed. E-mail: jahnwen@hotmail.com, Tel.: +86-15980856178

mainly investigate the impact of pressure on the index, structural properties and passivation of hydrogenated silicon nitride film by LF-PECVD.

## II. EXPERIMENTS

SiN<sub>x</sub>:H layers were prepared on polished wafers by direct low-frequency PECVD (40 kHz, Centrotherm) using NH<sub>3</sub> (99.998%) and SiH<sub>4</sub> (99.995%) as process gases. Single-sided polished P type CZ (Czoehral-ski) silicon wafers of resistivity 1 Ωcm were cut into 125 mm×125 mm to use. After a standard RCA (Radio Corporation of America) cleaning, SiN<sub>x</sub>:H layers were deposited on the substrates. The etching of the native oxide from the wafers by HF-based solution was carried out prior to the deposition of SiN<sub>x</sub>:H films. The pressure varied from 160 Pa to 280 Pa, while all other deposition parameters (temperature about 450 °C, ammonia-to-silane gas flow ratio about 4.2/0.5 L/min in standard cubic, plasma power about 810 W, and total gas flow) maintained constant. Every pressure group had the 10 pieces of wafers.

The thickness and refractive index of the SiN<sub>x</sub>:H films deposited with different pressures were measured by spectroscopic ellipsometry (Company: Sofra, France; Model: SOFRA-GEs) at laser wavelength of 633 nm. The effective minority carrier lifetime  $\tau_{\text{eff}}$  of the silicon substrate with the films was measured with microwave photo conductance decay (MWPCD) technique (Company: Semilab, Hungary; Model: WT2000). In order to investigate the pressure influence on the content of Si–H, N–H, and Si–N bond, the samples were studied with Fourier transform infrared (FTIR) spectroscopy (Company: Agilent, USA; Model: Varian Excalibur 3100).

## III. RESULTS AND DISCUSSION

### A. Film refractive index and density

The refractive index in the range of 2.017–2.082 are all suitable for the requirements of antireflection coating for silicon solar cells, and it has a little increase with the increase of the pressure as Fig.1 shows.

The refractive index is often used as an indication of the Si-content of the SiN<sub>x</sub>:H layers. As suggested by Lelièvre [16], the empirical equation observed by Dauwe are in good agreement with the results reported elsewhere for LF-PECVD reactor (40 kHz, Centrotherm) [17].

$$n = 1.22 + 0.61/x \quad (1)$$

where  $n$  is the refractive index,  $x=[\text{N}]/[\text{Si}]$  is mole ratio.

According to the Eq.(1) and results of refractive index in the Fig.1, we can infer that  $x$  is 0.71–0.77 that shows all the SiN<sub>x</sub>:H layers are silicon rich because  $x$  is about

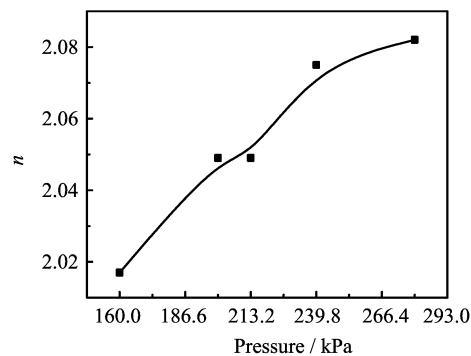


FIG. 1 Refractive index  $n$  of SiN<sub>x</sub>:H films deposited at different pressure.

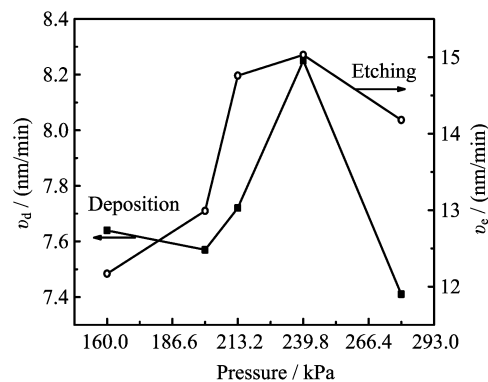


FIG. 2 Deposition rate ( $v_d$ ) and etching rate ( $v_e$ ) of SiN<sub>x</sub>:H films deposited at different pressure.

1.33 of silicon nitride molecular formula Si<sub>3</sub>N<sub>4</sub>. The Si content of the layers increased with the increase of the pressure, but the degree increased slightly. The reason is probably that the increasing pressure results in a decrease in electron energy, which subsequently leads to a decrease of NH<sub>3</sub> into SiH<sub>4</sub> radical ratio, namely the increase of Si/N ratio [15, 18]. This interpretation is also consistent with the enhanced concentration of N–H bonds resulting from a pressure decrease, as shown by the following analysis of FTIR transmission spectra.

The SiN<sub>x</sub>:H film were etched in 5% (mass ratio) HF solution to test the film density. The etching rate  $v_e$  and deposition rate  $v_d$  of the SiN<sub>x</sub>:H films with various pressure are shown in Fig.2.  $v_e$  curve shows inverse change of density of film with pressure. High deposition rate will induce loose SiN<sub>x</sub>:H film since the reactive particles have not enough time to re-locate at higher  $v_d$ . Therefore  $v_d$  and  $v_e$  have the same change trend with pressure as Fig.2 shows. They firstly increases with the increase of the pressure, then decrease when the pressure is equal to 240 Pa.

The pressure will affect the reaction from two sides: high pressure produces the high density of reactive gas SiH<sub>4</sub> and NH<sub>3</sub>, which can speed up the reaction rate. At the same time, high pressure can result in low electron energy, which can slow the reaction. Figure 2 shows

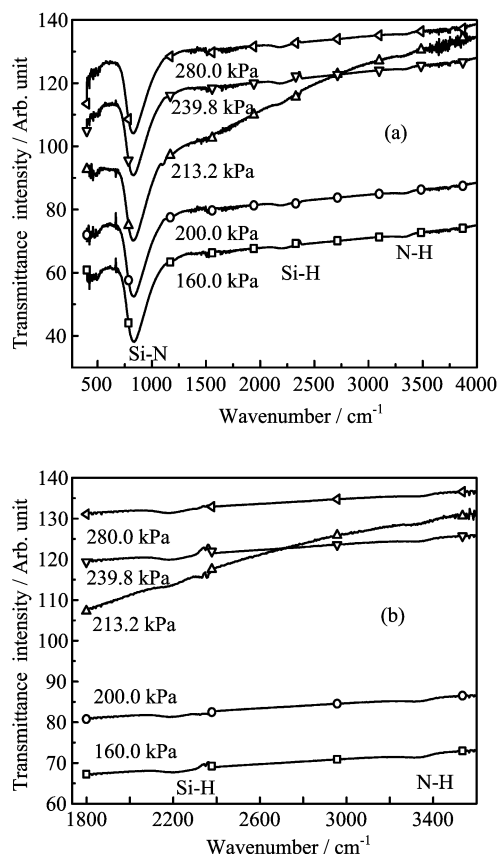


FIG. 3 FTIR transmission spectra of  $\text{SiN}_x\text{:H}$  films deposited at different pressures. (a) Si-N, Si-H, and N-H bond. (b) Si-H bond and N-H bond.

that firstly the  $v_d$  is mainly controlled by density of reactive gases and then by electron energy after 240 Pa pressure.

## B. Film structural properties

The initial content of hydrogen and the mass density in  $\text{SiN}_x\text{:H}$  film are considered as the key factors not only for bulk passivation, but also for the surface passivation. FTIR transmission spectra from 400  $\text{cm}^{-1}$  to 4000  $\text{cm}^{-1}$  for films prepared at different pressure are summarized in Fig.3. The intensity of different bonds absorption peak as shown in the FTIR transmission spectra was corrected for layer thickness. As well known, in  $\text{SiN}_x\text{:H}$  film the main vibrational modes in the FTIR peak appear at around 850  $\text{cm}^{-1}$  for Si-N stretching mode, 2140–2200  $\text{cm}^{-1}$  for Si-H bond stretching mode and 3330–3340  $\text{cm}^{-1}$  for N-H bond stretching mode respectively [19]. Different absorption bands associated to N-H bond at 3350  $\text{cm}^{-1}$ , and those caused by the Si-H bond at 2180  $\text{cm}^{-1}$ , together with the fundamental bond at 850  $\text{cm}^{-1}$  associated with the Si-N bond are observed in Fig.3.

As for hydrogen, the N-H bond vibration at

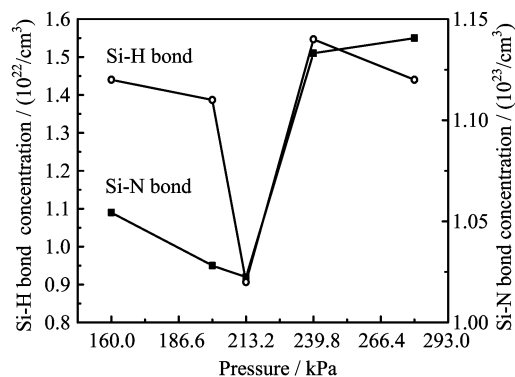


FIG. 4 Si-H and Si-N bond concentration of the  $\text{SiN}_x\text{:H}$  films deposited at different pressure.

3340  $\text{cm}^{-1}$  and the Si-H bond vibration around 2180  $\text{cm}^{-1}$  are the most important [20]. The total bonded hydrogen was calculated by adding the N-H and Si-H bond densities which were determined from FTIR spectroscopy using the method suggested by Landford and Rand [21].

The Si-N density was also calculated using FTIR spectroscopy according to the analysis as reported by Bustarrett *et al.* [22] and Giorgis *et al.* [23]. The Si-N bond is major product of reaction, which shows one order of magnitude larger than Si-H bond density and a decrease and then an increase with the pressure as shown in Fig.4. This is probably also the compromise result of two factors: high pressure can increase the concentration of reactants, especially  $\text{SiH}_4$  and at the same time decrease the electron energy that will affect the  $\text{NH}_3$  reaction strongly. It is interesting to notice that the Si-H bond density and the Si-N bond density followed the same trend as shown in Fig.4.

The Si-N bond densities of all the layers were greater than 10<sup>23</sup>/cm<sup>3</sup>. These results were bigger nearly an order of magnitude than those of the  $\text{SiN}_x\text{:H}$  film by Roth & Rau PECVD system [24]. For the remote method, the film forms after ion ionization and then spreads to the silicon surface. This fact leads to not only much less ion bombardment on the surface and high film growth rate [5], but also smaller mass density than the direct PECVD. The Si-N density is crucial for the thermal stability of surface passivation. ECN researchers have found that, Si-rich films may be better than N-rich, the final quality of Si-rich film after high temperature annealing is clearly superior to lower refractive index film (N-rich) [25]. The Si-N bond density is an important parameter for the diffusion of H, which is crucial for bulk passivation properties [26].

As can be seen from Fig.5, the concentration of N-H bond monotonic decreases with pressure and it is due to low pressure decreasing the electron energy, leading to less active  $\text{NH}_3$  and producing less N-H bonding [15]. The total density of H bond gotten from the sum of the Si-H and N-H bond is shown in Fig.5.

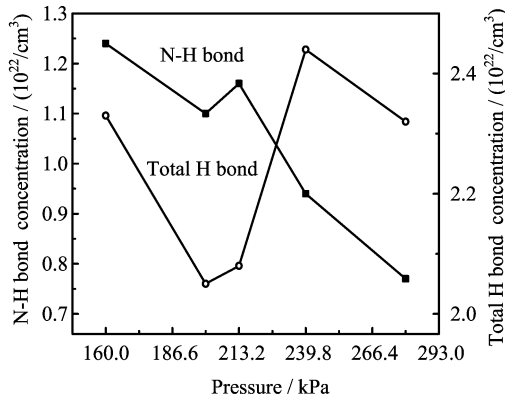


FIG. 5 The N–H bond and total H concentration of the SiN<sub>x</sub>:H films deposited at different pressure. The total density of H bond gotten from the sum of the Si–H and N–H bond.

### C. Surface passivation

The effective minority carrier lifetime of silicon wafer can be used as an characterization of the passivation effect, and the results of  $\tau_{\text{eff}}$  of the silicon substrate coated with the SiN<sub>x</sub>:H films tested by microwave photo conductance decay is shown in Fig.6. As we can see,  $\tau_{\text{eff}}$  became larger with increase of the pressure, and then drop with the pressure at middle pressure.

Comparing  $v_e$  in Fig.2 with  $\tau_{\text{eff}}$  in Fig.6, it is shown that the film with smaller density has higher  $\tau_{\text{eff}}$ . This conflict with the fact that large film density will induce good passivation. Therefore, film density is not the dominated passivation effect in these films.

The hydrogen in the film can diffuse into the silicon bulk to passivate dangling bond after the fast firing process. Therefore the H content in the film will have an influence on the bulk passivation. The total H bond density changing with pressure is shown in Fig.5. However it has a reversed change compared with  $\tau_{\text{eff}}$  changing with the pressure in Fig.6. That is to say, the H bulk passivation is also not the main passivation effect as the film density, while the field-effect passivation by Si dangling bond should be the dominating passivation.

The Si dangling bond is the dominant deep defect in SiN<sub>x</sub>:H films. Its predominant configuration is Si≡N<sub>3</sub> (the so-called K centre), which creates a high density of states in the middle of the gap [27]. The K centers, in their stable form N<sub>3</sub>≡Si<sup>+</sup> (K<sup>+</sup> centers), contribute primarily to the positive charge Q<sub>f</sub> on the Si/SiN<sub>x</sub>:H interface. These positive charges Q<sub>f</sub> can reflect the minor carrier holes to prevent them from combining in this interface. This field passivation is dominant effect comparing with H bond passivation in the interface.

Since the total silicon content of the layers changes little according to the result of  $x$ , the sum of Si–H and Si–N bond density had great influence on the density of Si dangling bond, then on the density of the positive charge Q<sub>f</sub>. The decrease of the sum of Si–H and Si–N

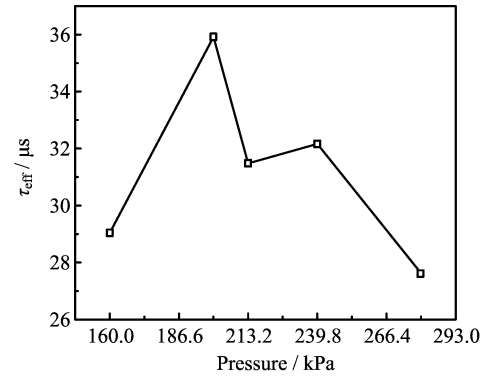


FIG. 6 The effective minority carrier lifetime  $\tau_{\text{eff}}$  of the silicon passivated with the SiN<sub>x</sub>:H films deposited at different pressure.

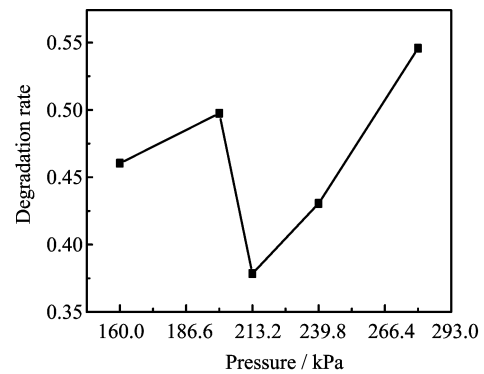


FIG. 7 The degradation rate of effective minority carrier lifetime of the silicon passivated with the SiN<sub>x</sub>:H films deposited at different pressure.

bond density in middle pressure (Fig.4) would result in the increase of the Si dangling bond, further lead to the increase of Q<sub>f</sub>. More effective field-effect passivation can be achieved with increase of Q<sub>f</sub>, which gives higher minority carrier lifetime just as shown in Fig.6. Figure 6 shows a contrary trend comparing with the Si–N and Si–H bond shown in Fig.4.

Unfortunately, degradation of passivation effect was observed, as is shown in Fig.7. The effective minority carrier lifetime was not stable until a month later. We can probably attribute the degradation to the breaking up of Si–H bonds at the Si/SiN<sub>x</sub>:H interface and/or within bulk of silicon by UV photons illuminating [28]. These interface Si–H bonds should have the same variable trend as the Si–H bonds in the film with degradation time. It can be imaged that high Si–H bond density in the film has large degradation. Therefore the degradation curve in Fig.7 have the same trend with Si–H bond trend in the Fig.4.

## IV. CONCLUSION

SiN<sub>x</sub>:H film with perfect anti-reflectance and passivation effect was obtained by direct low-frequency

PECVD (40 kHz, Centrotherm) using the mixture atmosphere of  $\text{NH}_3$  and  $\text{SiH}_4$  gas. The refractive index had a slow increase with the increase of the pressure. The pressure also had great influence on the Si, N, and H bonding structure in the  $\text{SiN}_x\text{:H}$  film. The  $\text{SiN}_x\text{:H}$  films prepared by direct LF-PECVD were very dense, with the Si–N bond densities greater than  $10^{23}/\text{cm}^3$ . The results also highlighted high hydrogen content. The concentration of N–H bond became smaller as pressure increased, while the Si–H bond density and the Si–N bond density following the same trend was the variations of the pressure: first decreasing and then increasing with the increase of the pressure. The passivation effect was greatly influenced by the Si dangling bond density. Degradation of passivation effect was observed, and was probably caused by the breaking of the Si–H bond density at the Si/ $\text{SiN}_x\text{:H}$  interface.

- [1] T. Jana, S. Mukhopadhyay, and S. Ray, *Sol. Energy Mater. Sol. Cells* **71**, 197 (2002).
- [2] J. F. A. Nijs, *Advanced Silicon and Semiconducting Silicon Alloy Based Materials and Devices*, 1st Edn., Bristol: Institute of Physics Publish, 323 (1994).
- [3] J. Nijs, J. Szlufcik, J. Poortmans, S. Sivotthaman, and R. P. Mertens, *Adv. IEEE Trans. on Electron Devices* **46**, 1948 (1999).
- [4] Z. L. Wen, X. L. Cao, C. L. Zhou, L. Zhao, H. L. Li, and W. J. Wang, *Acta Phys. Chim. Sin.* **27**, 1531 (2011).
- [5] F. Duerinckx and J. Szulfcik, *Sol. Energy Mater. Sol. Cells* **72**, 231 (2002).
- [6] B. Karunagaran, S. J. Chung, S. Velumani, and E. K. Suh, *Mater. Chem. Phys.* **106**, 130 (2007).
- [7] A. G. Aberle, *Crystalline Silicon Solar Cells: Advanced Surface Passivation and Analysis*, 1st Edn., Sydney: University of New South Wales Press, 106 (1999).
- [8] H. Mackel and R. J. Ludemann, *Appl. Phys.* **92**, 2602 (2002).
- [9] B. L. Sopori, X. Deng, J. P. Benner, A. Rohatgi, P. Sana, S. K. Estreicher, Y. K. Park, and M. A. Robertson, *Sol. Energy Mater. Sol. Cells* **41**, 159 (1996).
- [10] J. Hong, W. M. M. Kessels, W. J. Soppe, A. W. Weeber, W. M. Arnoldbik, and M. C. M. VandeSanden, *J. Vacuum Sci. Technol. B* **21**, 2123 (2003).
- [11] J. Schmidt and M. Kerr, *Sol. Energy Mater. Sol. Cells* **65**, 585 (2001).
- [12] W. Soppe, H. Rieffe, and A. Weeber, *Prog. Photovolt: Res. Appl.* **13**, 551 (2005).
- [13] G. Santana and A. Morales-Acevedo, *Sol. Energy Mater. Sol. Cells* **60**, 135 (2000).
- [14] J. Yoo, S. Dhungel, and J. Yi, *Thin Solid Films* **515**, 5000 (2007).
- [15] J. Wei, P. L. Ong, F. E. H. Tay, and C. Ilescu, *Thin Solid Films* **516**, 5181 (2008).
- [16] J. F. Lelièvre, E. Fourmond, A. Kaminski, O. Kaminski, D. Ballutaud, and M. Lemiti, *Sol. Energy Mater. Sol. Cells* **93**, 1281 (2009).
- [17] S. Dauwe, *Ph.D Thesis*, Hannover: Hannover University, (2004).
- [18] D. W. J. Hess, *Vac. Sci. Technol. A* **2**, 244 (1984).
- [19] D. V. Tsu, G. Lukovsky, and M. Mantini, *J. Phys. Rev. B* **33**, 7069 (1986).
- [20] A. Morimoto, Y. Tsujimura, M. Kumeda, and T. Shimizu, *J. Appl. Phys.* **24**, 1394 (1985).
- [21] W. A. Lanford and M. J. Rand, *J. Appl. Phys.* **49**, 2473 (1978).
- [22] E. Bustarret, M. Bensouda, M. C. Habrard, and J. C. Bruyere, *Phys. Rev. B* **38**, 8171 (1998).
- [23] F. Giorgis, F. Giuliani, C. F. Pirri, E. Tresso, C. Summonte, R. Rizzoli, R. Galloni, A. Desalvo, and P. Rava, *Phil. Mag. B* **77**, 925 (1998).
- [24] A. Cuevas, F. Chen, J. Ton, J. Tan, H. Mackel, S. Winderbaum, and K. Roth, *In 4th World Conference on Photovoltaic Energy Conversion*, Waikoloa, 1148 (2006).
- [25] A. W. Weeber, H. C. Rieffe, I. G. Romijn, W. C. Sinke, and W. J. Soppe, *The 31st IEEE Photovoltaic Specialists Conference*, Florida, 1043 (2005).
- [26] W. M. A. Bik, R. N. H. Linssen, F. H. P. M. Habraken, W. F. van der Weg, and A. E. T. Kuiper, *Appl. Phys. Lett.* **56**, 2530 (1990).
- [27] J. Robertson, W. L. Warren, and J. Kanicki, *J. Non-Crystalline Solids* **187**, 297 (1995).
- [28] R. Hezel and K. Jager, *J. Electrochem. Soc.* **136**, 518 (1989).